Cross sections for rotational decoherence of perturbed nitrogen measured via decay of laser-induced alignment

N. Owschimikow,[1,a)] F. Königsmann,[1] J. Maurer,[1,b)] P. Giese,[1] A. Ott,[1] B. Schmidt,[2] and N. Schwentner[1,c)]
[1]*Institut für Experimentalphysik, Freie Universität Berlin, Arnimallee 14, 14195 Berlin, Germany*
[2]*Institut für Mathematik, Freie Universität Berlin, Arnimallee 6, 14195 Berlin, Germany*

(Received 27 April 2010; accepted 23 June 2010; published online 30 July 2010)

We quantitatively determine cross sections for rotational decoherence from the decay of nonadiabatic laser-induced alignment in nitrogen and nitrogen-foreign gas mixtures in a temperature range between 80 K and room temperature. The cross section for rotational decoherence in pure nitrogen decreases from 102 $Å^2$ at 80 K to 48 $Å^2$ at 295 K, leading to long-lived coherences even at high temperatures. Comparison with the broadening of the transition lines of the Raman Q-branch reported in the literature shows that the decay of rotational coherence proceeds at the same rate as rotational depopulation. This is verified also for mixtures of nitrogen with hydrogen, helium, argon, and krypton. We discuss limits posed by a possible J-dependence of the cross sections and strategies for state resolved determination from the time-dependent alignment signal. © *2010 American Institute of Physics*. [doi:10.1063/1.3464487]

I. INTRODUCTION

During the recent decade, the nonadiabatic laser-induced alignment of molecules in the gas phase has gained major importance in many areas of ultrafast spectroscopy.[1,2] Beyond the study of the phenomenon itself, aligned ensembles of molecules are used to provide targets with well-defined spatial orientation for subsequent investigation or manipulation. These include the study of direction-dependent properties, e.g., ionization,[3,4] imaging of molecular orbitals through x-ray diffraction,[5,6] or the generation of high harmonics[7–10] on one hand and the use of aligned ensembles as tools, e.g., for the generation of attosecond laser pulses[11,12] or the shaping of femtosecond pulses.[13,14] In all these experiments, the so-called postpulse or field-free alignment[15] and rotational revivals are exploited. The postpulse alignment, being a consequence of the creation of rotational coherence in the molecular ensemble, shows the characteristic transient revival features typical for a quantum wave packet.[16] It is thus possible to study the aligned molecules without the interference of the additional external electric field used to generate the alignment. With the revival period governed by the least common multiple of the frequencies associated with the transitions excited, the motion of a rotational wave packet is a relatively slow process compared to the also widely studied vibrational or electronic wave packets.[17,18] Typical rotational revival times for diatomic molecules are 8.38 ps for the light nitrogen with a rotational constant of 1.989 cm^{-1}, or 450 ps for the heavy iodine molecule with a rotational constant of 0.037 cm^{-1}. The recurrences of rotational wave packets are an important field of research and a manifold of approaches has been developed for their manipulation[19–22] and even use in quantum information schemes.[23,24] All these processes require the persistence of rotational coherence in time, and this naturally leads to an interest in the time scales and mechanisms that lead to the decay of rotational coherence in the aligned ensemble.

Events causing the loss of coherence are separated into those initiating pure dephasing, while maintaining the population of the quantum state and those related to energy relaxation, i.e., the exchange of population between quantum states while the system is relaxing toward its thermal equilibrium state.[25] Referring to energy relaxation, one distinguishes further between the initial depopulation event of an excited level and the overall relaxation of the system under investigation to its thermal equilibrium. The initial collisional depopulation of rotational levels is addressed in experiments measuring the broadening of the rovibrational transition lines in the stimulated Raman Q-branch.[26–29] Another class of experiments determines the cross section for rotational relaxation by measuring the evolution of rotational temperature in a molecular beam[30,31] or ultrasound absorption in a gas flow.[32,33] The term relaxation rather than depopulation here refers to the return to thermal equilibrium, which may involve several inelastic collision events. The cross section σ^r characterizing the rotational relaxation is thus smaller than the cross section σ^p for rotational depopulation.[34] Coherence is destroyed in all collisions, elastic as well as inelastic ones, and one might thus expect the cross sections σ^c for rotational decoherence to be still larger than the cross sections for rotational depopulation. Rotational depopulation with σ^p is connected with a change ΔJ in the rotational quantum number J. Pure dephasing, i.e., elastic collisions, included in σ^c would require a change ΔM in the projection of J in alignment direction, without depopulation ($\Delta J=0$). In principle, both rates can be extracted from an

[a)]Electronic mail: nina.owschimikow@fu-berlin.de.
[b)]Present address: Department of Chemistry, University of Aarhus, DK- 8000 Aarhus C.
[c)]Electronic mail: nikolaus.schwentner@fu-berlin.de.

alignment experiment at high laser intensity.[35,36] In the binary collision regime, which holds for diatomic gases under ambient conditions, it is commonly assumed, however, that pure dephasing does not play any role.[37] The depopulation cross sections σ^p derived from Raman Q-branch line broadening experiments should therefore well correspond to the decay rates and decoherence cross sections σ^c observed in rotational coherence experiments.

Inelastic Raman methods have been developed and extensively used as a diagnostic tool for low temperature expansions in molecular beams and for combustion at high temperatures.[38–40] Numerical values for the depopulation cross section σ^p, and the relaxation cross section σ^r therefore are quite abundant in the literature, while quantitative measurements of σ^c are rather scarce. In this work, we complement the picture by systematically measuring the decoherence cross section σ^c in nitrogen and mixtures of nitrogen with hydrogen and several noble gases.

We induce alignment by a linearly polarized short laser pulse and detect the time-dependent modification of birefringence caused by recurrences of alignment in a homodyne detected optical Kerr effect experiment.[41,42] The method is similar to the Raman induced polarization spectroscopy[43] that has been used in pioneering studies of alignment decay in N_2, O_2, and CO_2 at room temperature.[44,45] The alignment dynamics in these experiment appeared to be well explained by a multiparameter scaling law analysis using state-resolved decay rates from Raman Q-branch experiments, suggesting that for these examples at room temperature the predicted equality between σ^p and σ^c holds. We show in our contribution that σ^c for nitrogen can be obtained in a straightforward way from the decay of the peak area of revivals in the homodyne detected optical Kerr effect signal, without resorting to any modeling. We discuss several advantages our approach presents over frequency-domain measurements for the use in diagnostics. In addition to experiments with pure nitrogen, we then employ a variety of light (He), medium (Ar), and heavy (Kr) atomic perturbers. For molecular perturbers we use nitrogen itself with its resonant rotational structure, and hydrogen with a much larger rotational constant. Temperatures in our experiments are varied between the liquefaction temperature of nitrogen around 80 K and room temperature, and pressures between 0.1 and 1 atm are comparable to atmospheric conditions. This presents a set of data that allows to systematically check the relation between the depopulation cross section σ^p and the decoherence cross section σ^c.

II. THEORY

The interaction of a linear diatomic molecule with the electric field of a linearly polarized laser is mediated via the electronic polarizability tensor α of the molecule. The potential the molecule experiences is determined by the difference in polarizabilities along the main axes of the molecule. For a diatomic molecule in an electronic Σ-state, $\alpha_\parallel$ parallel to the molecular axis is generally larger than $\alpha_\perp$ perpendicular to it, the molecule thus possesses an anisotropy of polarizability $\Delta\alpha=\alpha_\parallel-\alpha_\perp$. Far away from any resonance the potential in a rapidly alternating field is described within the rotating wave approximation as[46,47]

$$H_{\mathrm{ind}}(\theta,t) = -\tfrac{1}{4}\Delta\alpha E^2(t)\cos^2\theta - \tfrac{1}{4}\alpha_\perp E^2(t), \tag{1}$$

where θ is the angle the molecular axis forms with the polarization direction of the laser and E is the laser electric field amplitude. The observable characterizing the degree of molecular alignment is the ensemble-averaged expectation value $\langle\langle\cos^2\theta\rangle\rangle$ of the squared alignment cosine. We use $\langle\langle\ \rangle\rangle$ to refer to the values averaged over the thermal ensemble and $\langle\ \rangle$ for the quantities averaged for the wave packet originating from a pure quantum state. The complete Hamiltonian describing the nonresonant molecule-field interaction is the sum of the induced potential H_{ind}, the free rotor Hamiltonian H_0, and a dissipative term. Dissipation in rotational alignment was tackled theoretically in Refs. 35 and 36 based on the density matrix. We do not make use of the formalism developed in these publications, and apply the Hamiltonian for the isolated molecule-field system

$$H(t) = H_0 + H_{\mathrm{ind}}(t), \tag{2}$$

where

$$H_0 = B\mathbf{J}^2, \tag{3}$$

with

$$H_0|JM\rangle = (BJ(J+1) + DJ^2(J+1)^2)|JM\rangle. \tag{4}$$

Here, $\mathbf{J}$ denotes the angular momentum operator, B and D are the rotational and the centrifugal constants, respectively, and $|JM\rangle$ is a rotational eigenstate characterized by the angular momentum quantum number J and its projection onto the polarization direction M. The rotational quantum state of a molecule is usually expanded in terms of these states as

$$|\Psi_{JM}(t)\rangle = \sum_{J'M'} c^{(JM)}_{J'M'}(t)|J'M'\rangle, \tag{5}$$

where the time-dependence of the coefficients is accounting for the mixing of free rotor states during the pulse and where the initial conditions are given by $c^{(JM)}_{J'M'}(t=0)=\delta_{JJ'}\delta_{MM'}$. After the termination of the pulse $H_{\mathrm{ind}}=0$, and the dynamics is reduced to the analytical propagation of the coefficients for the functions representing the eigenstates of the free rotor. Calculations of alignment are performed numerically by various methods published, e.g., in Refs. 22 and 48. We use the solution of the time-dependent Schrödinger equation for every quantum state

$$\frac{i\hbar}{B}\frac{\partial}{\partial t}|\Psi_{JM}\rangle = \frac{H(t)}{B}|\Psi_{JM}\rangle, \tag{6}$$

with subsequent thermal averaging provided by the WAVEPACKET software package.[49]

In the nonadiabatic limit of alignment, the laser pulse is significantly shorter than the rotational period of the molecule. In this case, the molecular time scale is too slow to allow for a coherent reemission of the exciting field, and thus the rotationally excited molecules persist in their motion after the turn-off of the pulse, resulting in transient recurrences

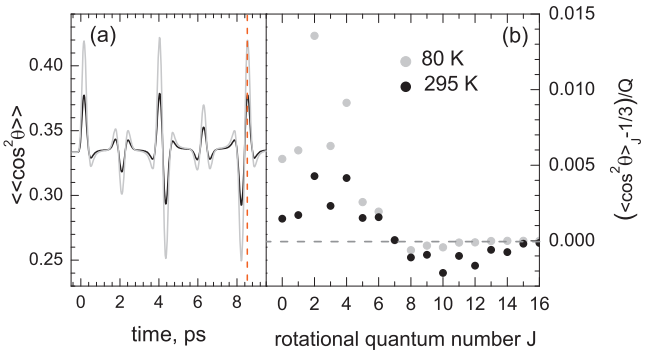

FIG. 1. (a) Numerical simulation of alignment in nitrogen upon the excitation with a Gaussian laser pulse of 150 fs FWHM duration and an intensity of 10 TW/cm^2 at 80 K (gray line) and 295 K (black line). (b) Deviation from the isotropic values in individual $|\Psi_J\rangle$ states at the time of the maximum of the full revival [dashed red line in (a)]. The zero deviation from 1/3 taken on in an isotropic ensemble is represented by the dashed horizontal line.

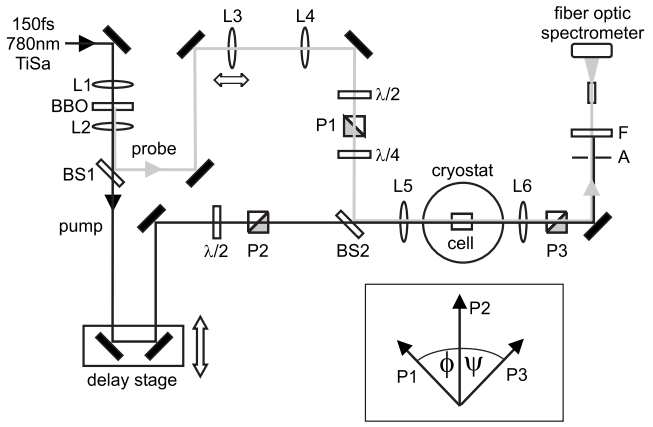

FIG. 2. Ultrafast optical Kerr effect setup with collinear geometry. L1 through L6: lenses, BBO: frequency doubling crystal, BS1 and BS2: dichroic mirrors, P1 through P3: Glan–Taylor polarizing prisms for probe (P1), pump (P2), and analyzer (P3), A: aperture, and F: colored glass filter. The inset shows the setting of polarizer axes with $\psi=-\phi=45°$ for maximum sensitivity.

of alignment in a rotational wave packet motion.[15] The period τ_r with which the alignment pattern repeats itself is given by the inverse of twice the rotational constant of the molecule, which is the least common multiple of rotational frequencies upon a Raman-type rotational excitation. In the case of nitrogen, one has $\tau_r=8.38$ ps.

Numerical simulations of alignment in nitrogen for the first revival period are displayed in Fig. 1(a) for temperatures of 80 K and 295 K. The wave packet motion results in a periodic oscillatory pattern in the degree of alignment $\langle\langle\cos^2\theta\rangle\rangle$ and a small increase of the time-averaged alignment beyond the isotropic value of 1/3 due to reorientation of molecular axes during the interaction with the laser pulse. Figure 1(b) shows the contributions of the individual $|\Psi_J\rangle$ states, i.e., the wave packets originating from the rotational level J. The symbols represent the deviation from the isotropic value for $\langle\cos^2\theta\rangle_J$ at the instant of the full revival maximum, shown by the dashed vertical line in part (a) of the figure. This value is given by $(\langle\cos^2\theta\rangle_J-1/3)$, the degree of alignment in one originally pure J state, divided by the sum over states $Q=\Sigma_J w_I(J)(2J+1)e^{-BJ(J+1)/kT}$. w_I here is a degeneracy factor due to the symmetry of the nuclear spin state, k is the Boltzmann constant, and T is the rotational temperature. For both temperatures, the distributions are rather similar and peak at $J=2$ and $J=4$, though at room temperature the maxima are less pronounced.

III. EXPERIMENT

We monitor the time evolution of rotational alignment by an ultrafast optical Kerr effect (OKE) method.[41] In this method, an anisotropy in the sample is detected by measuring the time delay-dependent elliptic component induced in a linearly polarized probe beam after passage through the sample that has been excited by a strong linearly polarized pump. We use a modification of the standard OKE setup[41] featuring collinearly propagating pump and probe beams that are discriminated spectrally rather than spatially, thus maximizing the interaction region by a large overlap of pump and probe.[50,51] The setup is schematically shown in Fig. 2. The excitation source is a commercial Ti-sapphire (Clark CPA 2001) amplified fiber oscillator (IMRA 780 femtolite) delivering pulses centered at 780 nm with a duration of 150 fs full width at half maximum (FWHM) and a repetition rate of 1 kHz. A fraction of the fundamental is frequency-doubled in a beta-barium borate (BBO) crystal to be used as a probe pulse and the two components are separated by a dichroic mirror (BS1). The delay between pump and probe is controlled by passing the pump over a linear delay stage. Glan–Taylor polarizing prisms are used to set the relative polarizations between pump and probe to an angle of 45° for maximal sensitivity. Probe polarizer and analyzer form a matched pair with a nominal extinction ratio of 5×10^{-6}. The half-wave plates in front of the polarizers act as continuously tunable filters allowing to adjust the intensity in both beams. A quarter-wave plate in the probe beam is used to compensate for spurious birefringence in the optical components. Pump and probe beams are overlaid by means of a dichroic mirror (BS2) and focused into the sample compartment by a lens with a focal length of 15 cm. This geometry yields a pump power density of up to 10 TW/cm^2 in the focus, and experiments were performed at typically 8 TW/cm^2. After the sample, the parallelized probe beam is filtered by an analyzer and the transmitted intensity is recorded by a fiber-coupled optical spectrometer with charge-coupled device (CCD) (Ocean Optics). An aperture and a colored glass filter in front of the detector suppress light from the pump and stray light due to spatially inhomogeneous spurious birefringence.

The sample is contained in a 3 cm long copper-enclosed cell attached to the cold finger of a bath cryostat (CryoVac) allowing to control the temperature between room temperature and 1.5 K. Our experiments are performed in a temperature range between 295 K and the liquefaction temperature of nitrogen at 77 K. For the experiments, we used nitrogen, hydrogen, helium, argon, and krypton gases all provided from Linde at pressures ranging between 0.1 atm up to 1 atm.

In a homodyne, or quadratic, detection scheme, probe polarizer and analyzer are crossed, yielding ideally no transmitted intensity in the presence of an isotropic sample. All

deviations from isotropy give rise to an elliptic component in the probe and thus a signal on the detector. The amount of ellipticity to be expected under our experimental conditions can be estimated from the phase lag accumulated by the probe electric field in the direction of the aligned molecular axes (extraordinary beam, e.o.) compared to the component perpendicular to it (ordinary beam, o.). With the wavelength in the sample being $\lambda_{o./e.o.}=\lambda/n_{o./e.o.}$, where λ is the vacuum wavelength and $n_{o./e.o.}$ is the respective refractive index, the probe beam accumulates a phase shift φ between ordinary and extraordinary component. The phase lag φ between o and e.o. components is given by

$$\varphi = \frac{2\pi\Delta n}{\lambda} z_0, \tag{7}$$

where $\Delta n = n_{e.o.} - n_{o.}$ is the difference in the refractive indices and z_0 is the interaction length in the direction of propagation z.

The refractive index of a gas at moderate densities can be approximated using the Lorentz–Lorenz equation[52] as $n \approx 1+2\pi N\alpha$, where N is the number density of molecules per unit volume and α is the polarizability. The maximal anisotropy of polarizability in the aligned ensemble is given by $\Delta\alpha\left(\langle\langle\cos^2\theta\rangle\rangle - \frac{1}{3}\right)$, where the anisotropy of polarizability is weighted by the degree of alignment achieved. The difference in refractive index for the probe beam is thus given by

$$\Delta n = 2\pi N\Delta\alpha\left(\langle\langle\cos^2\theta\rangle\rangle - \tfrac{1}{3}\right). \tag{8}$$

For nitrogen the number densities at atmospheric pressure at 295 K and 80 K are $N=2.4\times10^{19}$ cm^{-3} and $N=9.1\times10^{19}$ cm^{-3}, respectively. With the anisotropic polarizability of about 0.89×10^{-24} cm^3 (Ref. 53), the maximal possible Δn for perfect alignment equals $\Delta n_{max}=3.4\times10^{-4}$ for 80 K, and $\Delta n_{max}=8.7\times10^{-5}$ for 295 K. The maximal value for $\left(\langle\langle\cos^2\theta\rangle\rangle - \frac{1}{3}\right)$ that can be obtained under our experimental conditions is estimated from numerical simulations[49] to be about 0.087 at 80 K and 0.047 at room temperature, using a rotational constant of 1.989 cm^{-1} (Ref. 54) and power density of 10 TW/cm^2. The theoretical estimate for Δn under experimental conditions therefore yields 4.7×10^{-5} at 80 K and 0.61×10^{-5} at room temperature. The accumulated phase lag per unit length according to Eq. (7) thus amounts to $\phi/(z[\text{mm}])=44°/\text{mm}$ at 80 K, and 6°/mm at room temperature. With a collinear pump-probe geometry, the spatial overlap can be close to 1 mm. Depending on the quality of polarizers and the amount of spurious birefringence, thus a dynamic range of five orders of magnitude can be achieved in the experiment. To test this estimate, we determined the ellipticity induced in a linearly polarized probe pulse by 0.9 atm of nitrogen at a temperature of 80 K upon the excitation with a pump pulse of 160 fs duration and an intensity of 8 TW/cm^2. Extrapolating the above values to these conditions,[22] we arrive at a theoretical phase lag of 25°/mm. From the ratio of intensities measured for parallel and perpendicular setting of probe polarizer and analyzer, we derive an experimental phase lag of 13°. The length of the overlap region z_0 thus can be estimated to be about 0.5 mm long. The expansion of a light beam after the focus is described by[52] $w(z)=w_0\sqrt{(1+(z\lambda/\pi w_0)^2)}$, where w_0 is the radius of the beam waist in the focus, λ is the light wavelength, and z is the distance along the optical axis. With a beam waist of about 35 μm in the focus, determined by a scanning knife edge method, this corresponds to the beam diameter expanding by a factor of 2 over the distance of 0.5 mm, in accordance with the z_0 estimated using Eq. (7).

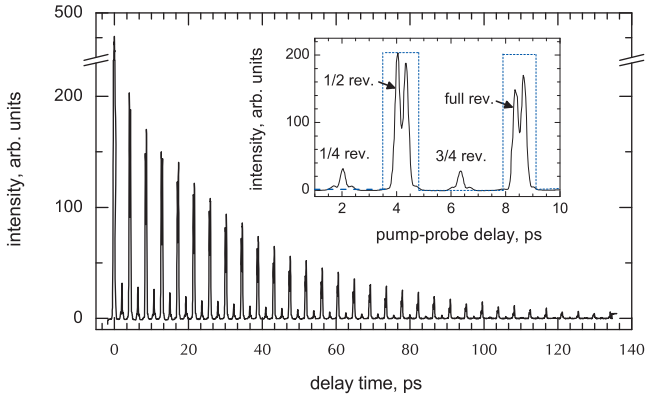

FIG. 3. Homodyne detected signal of alignment in pure nitrogen at 0.6 atm and 140 K. The inset shows a close-up of the first full revival period. The areas integrated over to determine the total intensities are outlined in blue.

The macroscopic detected intensity I_{hom} for the homodyne detection scheme is related to the microscopic observable $\langle\langle\cos^2\theta\rangle\rangle$ as[42]

$$I_{hom} \propto \left[\langle\langle\cos^2\theta\rangle\rangle(t) - \tfrac{1}{3}\right]^2. \tag{9}$$

All deviations from the isotropic orientation ($\langle\langle\cos^2\theta\rangle\rangle = 1/3$) cause a positive signal on the detector. Figure 3(a) shows a typical homodyne detected signal of rotational alignment in nitrogen. Revivals of rotational coherence show up as periodic maxima with a full revival period of $\tau_r = 8.38$ ps for nitrogen. In between full revivals, half revivals are observed with equal amplitude and opposite phase, and additionally quarter revivals displaying a smaller amplitude. The appearance of quarter revivals is a feature particular for homonuclear molecules, where odd and even rotational states are not equally populated due to nuclear spin statistics and the symmetry requirements for the total molecular wave functions.[21]

To quantify the decay of alignment in our experiments we used the integrated peak areas of half and full rotational revivals as indicated in the inset of Fig. 3(a). A change in shape of the revivals at long delays due to a decrease of B for large J numbers induced by the centrifugal distortion may be a point of concern. The ratio of the centrifugal energy correction to the rotational energy can be conveniently expressed as $(D_0/B_0^2)B_0J(J+1)$. The temperature of the sample determines the relevant rotational energies $B_0J(J+1)$, and the centrifugal parameter specific for the particular molecule is given by D_0/B_0^2. In nitrogen with $D_0/B_0^2=1.45\times10^{-6}$,[54] due to the stiffness of the triple bond the centrifugal correction to the rotational energy is relatively small, and thus the shape and amplitude of the revivals vary little with time, as is shown in the numerical simulation in the top trace of the inset in Fig. 4. For other molecules, this term can be higher, the extreme case being the hydrogen molecule[54] with

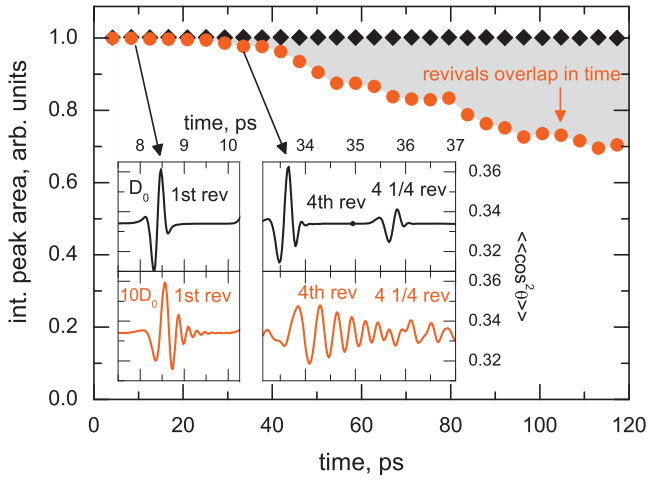

FIG. 4. Integrated peak areas of the half and full revivals of the simulated homodyne signal in $^{14}N_2$ at 300 K upon the excitation with a Gaussian laser pulse of 160 fs FWHM and 10 TW/cm^2 with the nitrogen centrifugal constant $D_0=5.67\times10^{-6}$ cm^{-1} (black diamonds) and an enlarged $D=10D_0$ (red circles). The insets show the shape and amplitude of the simulated alignment signal at the times of the first (left panel) and fourth (right panel) full revival for D_0 (top traces) and $10D_0$ (bottom traces).

$D_0/B_0^2=1.3\times10^{-5}$. We repeated the numerical simulation for nitrogen with the value for D_0 tenfold increased. The resulting alignment pattern is shown in the bottom traces of the inset of Fig. 4. The shape of the revivals is distorted by increasingly many trailing oscillations, as observed in Ref. 55 for the case of iodine, which starting from the fourth revival merge with the following quarter revival structures. The integrated peak area of the homodyne signal calculated according to Eq. (9) and displayed in Fig. 4, however, appears to be insensitive to changes in shape of the revivals as long as they can be clearly separated in time. The integrated peak area is thus an appropriate measure for the number density of molecules forming the rotational wave packet even in presence of centrifugal distortion.

IV. DECOHERENCE CROSS SECTIONS

A. Pure nitrogen

1. Temperature dependence

A plot of the integrated peak areas of half and full revivals for alignment in nitrogen at 0.9 atm pressure for four different temperatures between 95 and 280 K is displayed in Fig. 5. The solid lines are least-squares fits of single-exponential decays to the data, yielding a decay time τ_{exp}. For all temperatures, no systematic deviation from a single-exponential behavior is observed. This exponential decay is due to molecules being removed from the coherently rotating ensemble by random bimolecular collisions.

Measurements of alignment decay times τ_{exp} were performed in pure nitrogen in a temperature range between 80 K and room temperature for pressures between 0.1 and 3 atm. The normalized decay time $\tau_{hom}=\tau_{exp}/p$ derived from the observed decays did not show any dependence on the pressure p. The normalized lifetimes per unit pressure τ_{hom} in ps/atm for temperatures between 80 and 295 K are collected in Table I. τ_{hom} corresponds to half of the lifetime τ_c associ-

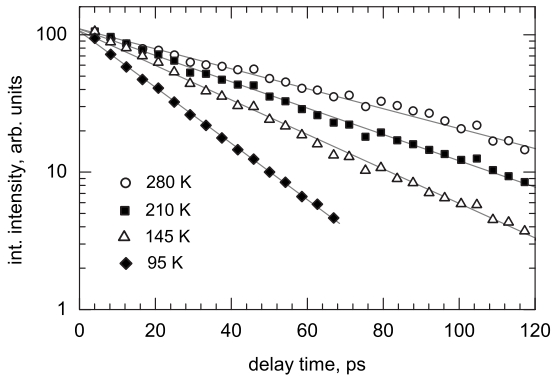

FIG. 5. Integrated revival peak intensities for homodyne detected alignment signals in pure nitrogen at 0.9 atm for various temperatures (open symbols). The solid lines represent least-squares fits of a single-exponential decay to the data.

ated with the decay of alignment, the difference being caused by the quadratic nature of detection according to Eq. (9). Figure 6 shows a plot of τ_{hom} as a function of temperature between 80 K and room temperature as solid symbols. The error bars in the plot are estimated from the scatter of a set of typically about five to ten individual measurements. Black symbols represent the experimentally determined τ_{hom} as a function of temperature normalized for a constant pressure of 1 atm. The gray symbols represent lifetimes as a function of temperature normalized for a constant number density in the gas volume. Though intuition tends to connect high temperatures with a rapid decay of coherence, and this is indeed true, e.g., for effects depending on electronic coherence, we observe an increasing lifetime of rotational coherence with increasing temperature. τ_{hom} grows from 14 ps/atm at 80 K to 64.5 ps/atm at 295 K (black symbols in Fig. 6). To exclude the influence of the reduced number density in the gas upon heating we normalized the data to the number density corresponding to 1 atm at 80 K (1.5×10^{-4} mol/cm^3). Thus normalized, the lifetimes for rotational coherence become almost independent of temperature, ranging from 14 ps at 80 K to 17 ps at 295 K (gray symbols in Fig. 6). The longer lifetime is observed despite the higher frequency of collisions one would expect from a higher translational velocity. This clearly shows that the cross section for a collision is temperature-dependent and decreases with increasing temperature.

TABLE I. Decay times of the homodyne detected alignment signal τ_{hom} in ps/atm and the cross section for rotational decoherence $\sigma^c_{N_2-N_2}$ derived from τ_{hom} in pure nitrogen between 80 and 295 K.

T (K)	τ_{hom} (ps/atm)	$\sigma^c_{N_2-N_2}$ (Å^2)
80	15.6 ± 2.5	102 ± 5
95	18.4 ± 2.5	94 ± 5
115	22.6 ± 2.5	84 ± 4
146	29 ± 3	74 ± 6
210	38.7 ± 3	66.5 ± 6
232	47.9 ± 4	56.5 ± 6
280	58.6 ± 4	51 ± 7
295	64.5 ± 5	48 ± 8

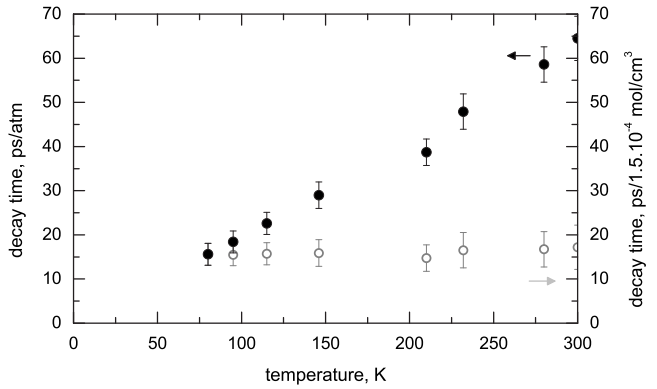

FIG. 6. Dependence of lifetime τ_{hom} of the homodyne detected alignment signal on temperature for pure nitrogen. Black symbols: τ_{hom} per constant pressure. Gray symbols: τ_{hom} for constant number density (corresponding to 1 atm at 80 K).

To further quantify these results we use the measured decay rates to calculate cross sections for rotational decoherence via a mean-free path model. In the following we analyze pure nitrogen as well as nitrogen-foreign gas mixtures. We therefore give the derivation of the cross section in its general form, for a mixture of different particle species with different properties. The frequency ν_{A-B} of collisions of a particle of species A with collision partners of species B leading to alignment decay within a unit time t is given by[56]

$$\nu_{A-B} = \frac{1}{\tau_c} = \frac{\pi(r_A + r_B)^2 \langle v_{\text{rel}} \rangle}{N_B/V}, \tag{10}$$

where N_B is the number of particles of species B in a volume V, r_A and r_B are the radii associated with the two species, and $\langle v_{\text{rel}} \rangle = \sqrt{\langle v_A^2 \rangle + \langle v_B^2 \rangle}$ is their relative velocity. For the average velocity $\langle v \rangle$ the mean velocity $\bar{v} = \sqrt{8kT/\pi m}$, with T being the temperature, m the molecular mass, and k the Boltzmann constant, is substituted.[57,58] In the older literature, sometimes also the most probable velocity $v_p = \sqrt{2kT/m}$ can be found,[28,59] as a result of which the calculated collision rates differ by a factor of $2/\sqrt{\pi}$. Equation (10) can thus be rewritten for the collision cross section σ_{A-B} using additionally the ideal gas law $N_B/V = p_B/kT$ as

$$\sigma_{A-B} = \pi(r_A + r_B)^2 = \frac{\nu_{A-B} kT}{\langle v_{\text{rel}} \rangle p_B}. \tag{11}$$

After inserting the expression for the relative velocity, eventually two formulas for the collision cross section for identical and foreign gas collisions can be derived

$$\sigma_{A-A} = \frac{\nu_{A-A}\sqrt{\pi m k T}}{4 p_A}, \tag{12}$$

$$\sigma_{A-B} = \frac{\nu_{A-B}\sqrt{\pi \mu k T}}{\sqrt{8} p_B}, \tag{13}$$

where $\mu = m_A m_B/(m_A + m_B)$ is the reduced mass of particles A and B.

For a pure gas, collision cross sections can be extracted from the decay rates of the measured alignment signal just by substituting the measured decay rate $1/\tau_c$ into Eq. (12). In a gas mixture, collisions with identical as well as with foreign gas particles contribute to the decay of the signal. Here, the rates of collision add up to yield the measured decay rate $\nu_{\text{tot}} = \nu_{A-A} + \nu_{A-B}$. The cross section σ_{A-B} can be extracted by performing a series of measurements in which the partial pressure of species A is kept constant. σ_{A-B} is then contained in the slope of a plot of ν_{tot} as a function of p_B, the intercept corresponding to ν_{A-A}.

Our method of detection was homodyning, i.e., quadratic detection. For homodyne detection, the signal integrated area depends quadratically on the number density of molecules in the coherently rotating ensemble. We verified this quadratic dependence of signal intensity on sample pressure for a range of pressures between 0.1 atm and 4 atm. To account for the effect of this dependence on the decay, a factor of 2 has to be introduced in going from τ_{hom} to τ_c to convert the decay rate ν_{hom} of the homodyne detected signal to the rate ν_{tot} at which particles are removed from the coherent ensemble ($\nu_{\text{hom}} = 2\nu_{\text{tot}}$).

The decays of the homodyne detected signal in our alignment experiments cover up to 2.5 orders of magnitude, and within this range showed no systematic deviation from a single-exponential decay. This indicates that the collision cross sections only weakly depend on the observed J quantum states. Strong variations with J would lead to a multiexponential decay. Numerical simulations using the decay rates from Ref. 26 showed a single-exponential decay of the simulated homodyne signal over more than three orders of magnitude, in agreement with our experimental observation. We made an estimate of the limits on the J-dependence of cross sections for our experimental conditions by numerical simulations of the decay of the homodyne detected signal over a delay time range of 120 ps. A deviation from a single-exponential decay resulted upon a 25% variation of the time constant for one of the significantly populated rotational levels or for imposing an overall gradient of more than 15% with J.

Though the dynamic range in our experiment can in principle be increased to resolve the slowly decaying tail due to a J-dependence of the decoherence rates, the obtained distribution of lifetimes is not linked to the distribution of rotational levels. To obtain state-resolved results from time-dependent experiments, one could resort to Fourier transformation of a heterodyne detected alignment signal and extract state-dependent lifetimes from the linewidth of the Fourier components. The Fourier transform method, however, requires to cover long delays in order to resolve the line shape of the components. In a recent publication,[22] we proposed a method to manipulate the state composition of a rotational wave packet by applying appropriately shaped single or double laser pulses. It is thus possible to create wave packets that are "hot" or "cool" compared to the environment, which is left at its original temperature. The method could be used to achieve state resolution in the analysis of rotational decoherence, isolating individual J states and determining their respective τ_{hom}.

We again emphasize that in this work, we report only decays that do not show a systematic deviation from a single-exponential behavior. This means that within the lim-

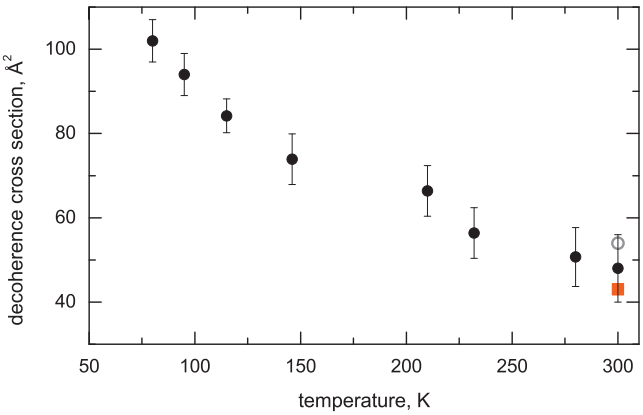

FIG. 7. Cross sections σ^c for rotational decoherence derived from the decay times of Fig. 6 vs temperature. The red square denotes the gas kinetic cross section of 43 Å^2 (Ref. 58), and the gray circle denotes the cross section σ^p for the $J=2$ rotational level of 57 Å^2 from Raman Q-branch measurements (Refs. 26 and 27).

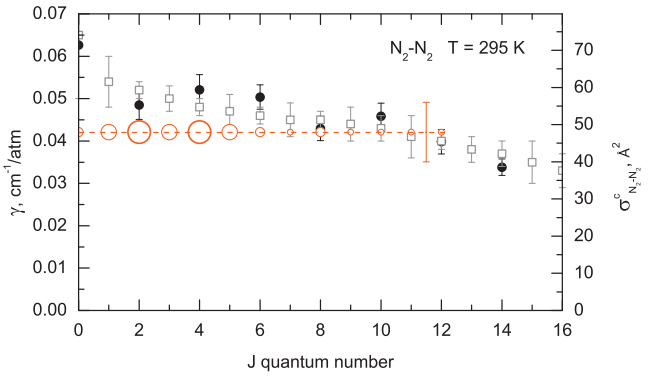

FIG. 8. Line broadening coefficients γ (HWHM) and $\sigma^p_{N_2-N_2}$ for the Raman Q-branch from Ref. 26 (gray symbols) and Ref. 27 (black symbols) for nitrogen at 295 K compared to our result for the $\sigma^c_{N_2-N_2}$ cross section (dashed red line). The size of the open circles corresponds to the weight of the particular state in the total alignment signal.

its of our accuracy discussed above τ_{hom} is independent of the rotational level. This statement holds for the range of rotational levels from $J=0$ to 6, which are relevant to our observations according to the weight distribution of Fig. 1(b). We indicate the relative contributions of the respective rotational level to our detected alignment signal by the size of the symbols in Fig. 8 and Figs. 10–13.

High velocities at high temperatures lead to more frequent encounters between molecules, and thus one would expect that an increased rate of collisions leads to a faster decay of the observed signal. In Fig. 6, we already showed that this is not the case for pure nitrogen, and that for a constant number density the lifetime of coherence becomes almost independent of temperature. The only term that can balance the increase in velocity in Eq. (10) to cause a nearly constant rate of decoherence, is the decoherence cross section σ^c of the molecules. Figure 7 shows the decrease in σ^c with increasing temperature derived from our experiments. The value determined at room temperature within the error margins coincides with the gas kinetic cross section (red square in Fig. 7) and thus the geometric size of the molecule. The cross section σ^p for rotational depopulation derived from the measurements of line broadening of the Raman Q-branch in Ref. 26 for the $J=2$ rotational level is plotted as a gray circle. From the quantitative agreement we conclude in agreement with previous results[37,44] that pure dephasing, i.e., elastic collisions, does not play a significant role in diatomic gases under ambient conditions.

The cross sections for decoherence σ^c derived from our experiments increase from 48 Å^2 at 295 K to 102 Å^2 at 80 K. The values for τ_{hom} and $\sigma^c_{N_2-N_2}$ are collected in Table I. An increase with decreasing temperature is observed experimentally also in rotational depopulation cross sections at high temperature,[60] as well as in rotational relaxation cross sections[30,31] for pure nitrogen. Reference 61 gives a theoretical analysis of line broadening coefficients by the energy corrected sudden (ECS) exponential power analysis, in which several temperature-dependent parameters are used to describe the behavior of the rotational depopulation. The main contributions are found to be the maximum angular momentum that can be transferred between rotational and translational degrees of freedom in a collision, which is proportional to the translational temperature, an amplitude factor accounting for density, which scales as $(T/T_0)^{-\beta}$ and the interaction time, approximately proportional to the inverse of the square root of the temperature. For different scaling laws, however, different sets of parameters, which are additionally interdependent, can be found in the literature to describe the observed cross sections. In our experiments at different temperatures, the main changes are in the rotational J-composition of the thermal ensemble, and in the distribution of translational energy. We conclude, based upon the fact that the rotational levels observed in the alignment signal do not significantly vary [Fig. 1(b)] that low translational velocities are responsible for high cross sections at low temperature. This suggests that orbiting collisions[62–64] are important at low temperature. The good reproduction of existing σ^p values by theory suggests that this qualitatively strong effect is implicitly contained in the calculations, though the frequently used interdependent parameters make it difficult to pinpoint the dominating physical mechanism.

2. Comparison with J resolved line broadening of Raman Q-branch at room temperature

The standard way to determine depopulation of rotational levels is the measurement of the pressure-dependent line broadening of the stimulated Raman Q-branch. In experiments of this kind a line broadening coefficient γ in cm^{-1}/atm, which additionally depends on temperature, is determined. In the line broadening coefficient, the frequency of inelastic collision events is expressed.[28,29] The method provides a J-resolution that stems from the very small change in the moment of inertia with the rotational quantum number due to centrifugal distortion of the molecular bond. Results of measurements in nitrogen at room temperature from Refs. 26 and 27 are plotted in Fig. 8 as gray and black symbols, respectively. The Q-branch method allows for rotational state resolved determination of depopulation rates. The line broadening coefficients vary from 0.054 cm^{-1}/atm for $J=1$ to

0.03 cm^{-1}/atm for $J=18$, where the numerical value refers to the half width at half maximum (HWHM) of the transition line.

For a quantitative comparison of these state-resolved coefficients with our cross section derived from the single-exponential decay, we plot in Fig. 8 the result obtained by us for a temperature of 295 K as a dashed horizontal line. Red circles of different sizes represent qualitatively the magnitude of the contribution of the particular rotational state to the alignment signal as it was estimated from Fig. 1(b). At room temperature, the alignment revivals appear to be dominated by low J states, especially the $J=2$ and $J=4$ rotational levels [Fig. 1(b)]. The thermal distribution of molecules has its maximum around $J=10$; however, the interaction mechanism of the molecular alignment favors high amplitudes in low J levels. Odd rotational states are twice less populated and therefore generally less visible. The error bar for the averaged value is derived from the scatter of several independent measurements.

For better comparison, we recalculated our measured decay times also into the units of γ via $\gamma=1/2\pi\tau_c$ (Ref. 29) assuming a Lorentzian line shape. The σ^c-axis in Fig. 8 gives the values for cross sections derived from the decay time τ_c, where a single-exponential decay was assumed. The requirement for comparison with the Raman Q-branch and the calculation of σ^p is that the line shape be a Lorentzian. We determine a decoherence cross section $\sigma^c_{N_2-N_2}$ of 48 $Å^2$ from a decay constant of 129 ps/atm for the alignment (64.5 ps/atm for the homodyne detected signal), which corresponds to a line broadening coefficient $\gamma=0.042$ cm^{-1}/atm.

In the range between $J=2$ and $J=6$, the line broadening coefficient reported in Ref. 27 decreases from 0.052 cm^{-1}/atm to 0.046 cm^{-1}/atm, corresponding to a depopulation cross section of 58 and 54 $Å^2$, respectively. Reference 27 reports an increase from 55 to 57 $Å^2$ and states excellent agreement with Ref. 26. This is consistent with the single-exponential decay observed in our experiments. Within the error bars of ± 8 $Å^2$, our cross section for decoherence of 48 $Å^2$ agrees well with the average value of 56 $Å^2$ from Refs. 26 and 27. It is not clear, whether our somewhat lower value presents a significant deviation, keeping in mind that it falls into a range, where the deconvolution of superimposed lines is necessary in the Raman experiments. For pure dephasing, however, one would expect that the cross section for decoherence σ^c exceeds the cross section for depopulation σ^p. This is evidently not borne out by our experiments. For pure nitrogen, our results confirm that decoherence proceeds via inelastic population transfer and the rate of pure dephasing by elastic collisions is negligible.

B. Nitrogen-foreign gas mixtures and comparison with Raman Q-branch data

1. Nitrogen-hydrogen

For the mixture of nitrogen and hydrogen a series of experiments were performed at a temperature of 77 K varying the pressure of hydrogen between 0.2 and 0.8 atm with a constant nitrogen pressure of 0.1 atm. Though hydrogen as a diatomic molecule with an anisotropy of polarizability can show alignment itself,[65] in our case the pulse duration is long compared to the hydrogen rotational period of 90 fs, and thus the nonadiabatic alignment dynamics in hydrogen is suppressed. We additionally verified the absence of a contribution from hydrogen by measurements on a hydrogen-filled cell. The signal detected originates exclusively from the nitrogen fraction in the mixture. The integrated peak areas of the homodyne signal for a series of measurements with 0.2, 0.4, and 0.8 atm hydrogen partial pressure are shown in Fig. 9 together with least-squares fits of single-exponential decays.

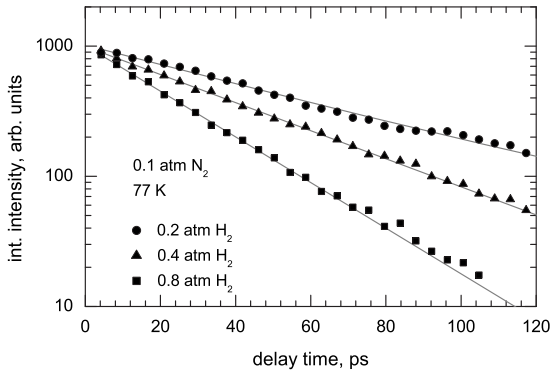

FIG. 9. Decay of integrated peak area of the homodyne detected signal vs time in a mixture of nitrogen and hydrogen at 77 K with varying hydrogen pressure (solid symbols). The solid lines are least-squares fits of single-exponential decays to the data.

The decay rate at 77 K depending on H_2-pressure was found to be $\nu^c_{N_2-H_2}=0.022$ ps^{-1} atm^{-1}, corresponding to a decay time of alignment of $\tau_c=51.3$ ps (102.6 ps^{-1} atm^{-1} for the homodyne detected signal) and a cross section $\sigma^c_{N_2-H_2}$ for dephasing of 22.1 $Å^2$. To obtain these values, the decay rates ν_{tot} measured in the nitrogen-hydrogen mixture were corrected by the pure nitrogen contribution of 0.0038 ps^{-1} for 0.1 atm of nitrogen at 77 K extrapolated from the values of Fig. 6 and Table I and subsequent averaging over the series of hydrogen measurements.

We observed no systematic dependence of the normalized decay rate on the hydrogen partial pressure. In Ref. 66, the authors calculate the depopulation rates for the N_2-hydrogen system. They differentiate in the calculation between para-hydrogen, which at low temperature is predominantly in the spherical $J=0$ rotational state and ortho-hydrogen, which mostly populates the $J=1$ rotational level and displays quadrupole-quadrupole interaction. Unfortunately the authors do not comment on the difference this fact may have on the cross sections. In addition to experiments with normal hydrogen, we employed an ortho-para hydrogen converter and carried out measurements with 99.8% pure para-hydrogen. Within our experimental accuracy, the decay rates in mixtures of nitrogen with normal and para-hydrogen did not show a significant difference.

For the nitrogen-hydrogen gas mixture, results of Raman Q-branch line broadening experiments at 77 K have been published in Ref. 66. The values obtained are plotted as black symbols in Fig. 10 together with the averaged cross section, we derive from our data at the same temperature (red dashed line). As in Fig. 8, the size of the red symbols signi-

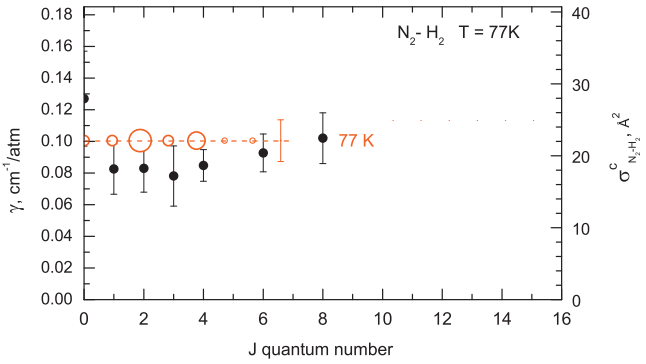

FIG. 10. Line broadening coefficients γ (HWHM) for the Raman Q-branch from Ref. 66 (black symbols) for a mixture of nitrogen and hydrogen at a temperature of 77 K compared to the values derived from the alignment decays measured at 77 K (red horizontal line). The size of the red symbols corresponds to the weight of the particular state in the total alignment signal.

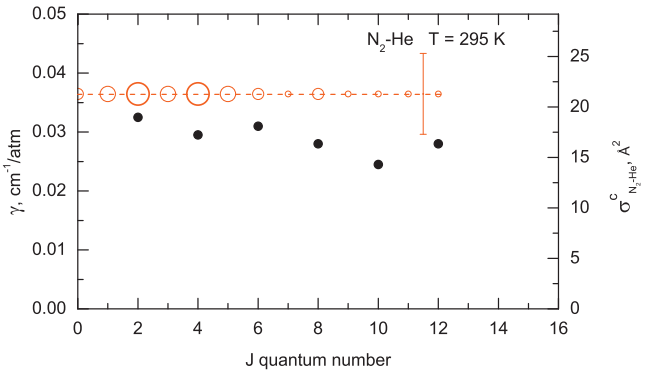

FIG. 11. Line broadening coefficients γ (HWHM) for the Raman S-branch from Ref. 72 (black symbols) for a mixture of nitrogen and helium at a temperature of 295 K compared to the cross section σ^c from the alignment decay (horizontal line). The size of the red symbols corresponds to the weight of the particular state in the total alignment signal.

fies the relative contribution of the respective rotational level to the detected alignment signal. Under our experimental conditions, the alignment signal at both room temperature and 77 K is mainly determined by small J numbers, especially the $J=2$ and $J=4$ rotational levels and should therefore be compared with the corresponding literature values. The error bar for our value is estimated from the scatter of a number of individual experiments.

The cross section $\sigma^c_{N_2-H_2}$ determined by us for the nitrogen-hydrogen mixture at 77 K is a bit larger than the Raman Q-branch line broadening coefficients determined in Ref. 66 but still lies within the error bars of the literature measurements. The average of the experimental broadening coefficient γ from Ref. 66 is about 0.08 cm^{-1}/atm, compared to our value of 0.1 cm^{-1}/atm, which amounts to a difference of 20%. The experimental depopulation rates of Ref. 66 have been found to be in excellent agreement with close-coupling theory based on *ab initio* quantum chemical potentials[67] and an ECS theory.[68] The reason for the discrepancy could be a small fraction of elastic collisions, or reorientation without depopulation, in the nitrogen-hydrogen system. Elastic depolarization has been reported in the literature for various polar molecules as OH (Refs. 69 and 70) and NO,[71] the rates for elastic encounters, however, have been found to be low for light collision partners and significant only for mixtures with argon and xenon.

2. Nitrogen-helium

Alignment experiments on the nitrogen-helium gas mixture were performed at room temperature at a constant partial pressure of nitrogen of 0.3 atm and at 80 K at 0.1 atm nitrogen pressure. The pressure of helium was varied between 0.4 and 3 atm.

At room temperature we determine a decoherence rate $\nu^c_{N_2-He}$ of 0.007 $ps^{-1}\,atm^{-1}$, corresponding to an alignment decay time τ_c of 143 ps/atm or a τ_{hom} of 71.5 ps/atm for the homodyne detected signal. The values were derived from averaging over a series of measurements with different partial pressures of helium after correcting for the decoherence rate of 0.0024 ps^{-1} estimated from Fig. 6 for 0.3 atm of nitrogen. The rate of decay translates into a cross section $\sigma^c_{N_2-He}$ of 21.3 $Å^2$.

At 80 K we measure a decay time for the homodyne signal τ_{hom} of 43.7 ps/atm, corresponding to $\nu^c_{N_2-He}$ of 0.0114 $ps^{-1}\,atm^{-1}$ or a cross section $\sigma^c_{N_2-He}$ of 18.1 $Å^2$. As opposed to pure nitrogen, here we observe a small increase in the cross section with temperature. An increase of the collision cross section with the temperature is also known in the literature for the N_2-H_2 system, with hydrogen and helium being very close in size and weight. From the line broadening data of the Raman Q-branch published for N_2-H_2 in Ref. 66, one can calculate a cross section $\sigma^p_{N_2-H_2}$ of 17.7 $Å^2$ for the $J=2$ rotational level at 77 K, growing to 19.4 $Å^2$ at 298 K and even 28.4 $Å^2$ at 580 K. The increase in $\sigma^{p/c}$ with decreasing temperature observed for pure nitrogen therefore does not seem to be a universal appearance but does depend on the system under investigation.

Experimental data on Raman line broadening in the nitrogen-helium system are limited to values for the Raman S-branch in Ref. 72 and are plotted in Fig. 11 as black symbols together with our averaged cross section. Again, the line broadening coefficients can be well accounted for by a scaling theory.[73] As in the case of hydrogen, our estimated value for γ of 0.037 cm^{-1}/atm is slightly larger than the 0.033 cm^{-1}/atm for the dominating $J=2$ contribution in the Raman S-branch line broadening.

3. Nitrogen-argon

For the nitrogen-argon gas mixture we performed measurements of alignment decay at 90 K and at room temperature. At low temperature a constant partial pressure of nitrogen of 0.1 atm was diluted by a variable partial pressure of argon between 0.2 and 0.8 atm. At 90 K we determine a signal decay time τ_{hom} of 22.7 ps/atm, corresponding to a collision rate of ν_{N_2-Ar} of 0.022 $ps^{-1}\,atm^{-1}$ and a cross section for decoherence $\sigma^c_{N_2-Ar}$ of 80.5 $Å^2$.

At room temperature, the nitrogen partial pressure was kept at 0.3 atm, and the argon pressure was varied between 0.4 and 3.2 atm. We obtain a collision rate ν_{N_2-Ar} of

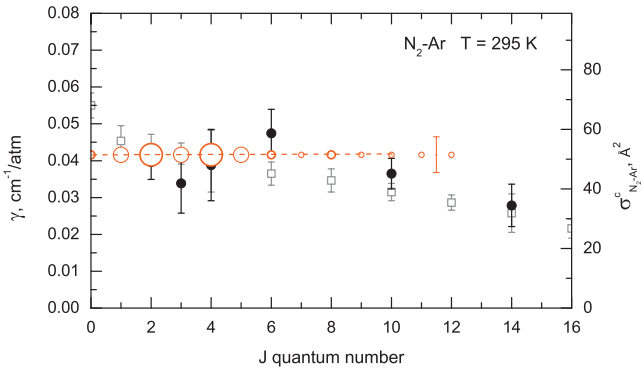

FIG. 12. Line broadening coefficients γ (HWHM) for the Raman Q-branch from Ref. 74 (black symbols) and Ref. 75 (gray symbols) for a mixture of nitrogen and argon at a temperature of 295 K compared to the cross section from the alignment decay (horizontal line). The size of the red symbols corresponds to the weight of the particular state in the total alignment signal.

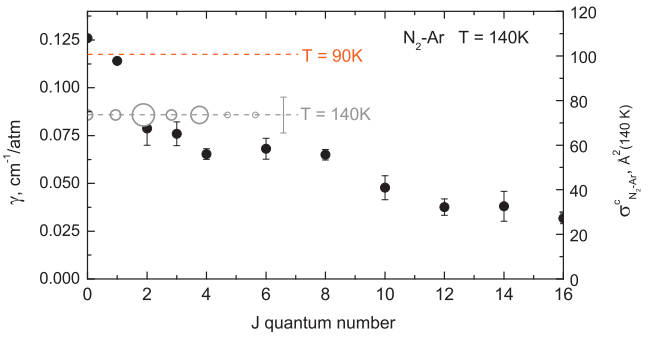

FIG. 13. Line broadening coefficients γ (HWHM) for the Raman Q-branch from Ref. 74 (black symbols) for a mixture of nitrogen and argon at a temperature of 140 K compared to the cross section $\sigma^c_{N_2-Ar}$ from the alignment decay measured at 90 K (red horizontal line) and extrapolated to 140 K (gray horizontal line). The size of the red symbols corresponds to the weight of the particular state in the total alignment signal.

0.0077 ps^{-1} atm^{-1}, which corresponds to a decay time τ_{hom} of 65 ps/atm in the experiment or a decoherence cross section σ_{N_2-Ar} of 51.1 $Å^2$. The collision rates and decay times seem surprisingly close to the ones measured for pure nitrogen and the nitrogen-helium mixture, given the difference in size between helium/argon and nitrogen molecules. This can be understood in a qualitative way, as the decay rate is determined by the size of the molecule through its cross section as well as by the frequency of encounters between molecules. Though argon has a much larger cross section than helium, the higher average velocity of the light helium molecules leads to more frequent encounters with nitrogen and thus a comparable decay rate at equal pressure of the rare gas. The pronounced temperature dependence of the decoherence cross section that was observed in pure nitrogen also becomes manifest in the mixture of nitrogen with argon.

Results of line broadening measurements of the Raman Q-branch for the nitrogen-argon system have been published in Ref. 74 and Ref. 75 for 140 and 295 K. In Fig. 12, results for γ of Ref. 74 (black symbols) and Ref. 75 (gray symbols) at room temperature are displayed in comparison with the averaged cross section $\sigma^c_{N_2-Ar}$ of 51.1 $Å^2$ derived from the alignment decay. The average line broadening coefficient γ from the literature values at $J=2$ is about 0.04 cm^{-1}/atm, and our cross section corresponds to a γ of 0.041 cm^{-1}/atm, in perfect agreement with the literature values. At room temperature therefore, the decay of coherence in the nitrogen-argon system can be explained by rotational depopulation. It should be noted that in Ref. 74, a theoretical description of depopulation rates based on potentials from Refs. 76 and 77 was attempted, which captured well the shape of the dependence of γ on J, but underestimated the rate severely. The same problem also appeared for the theoretical description of the depopulation rates at 140 K.

The literature data for the Raman line broadening at low temperature are limited to a temperature of 140 K, whereas our measurements were performed at 90 K. For pure nitrogen the cross sections in Fig. 7 show a decay with increasing temperature that can be approximated by a straight line. If one assumes a similar monotonic decay for the N_2-Ar system, the cross section at 140 K can be estimated from a linear interpolation between 90 and 300 K. The resulting comparison of literature values from Ref. 74 (black symbols) with our value (gray dashed line) is displayed in Fig. 13. Our original data at 90 K yield a γ of 0.117 cm^{-1}/atm and are shown as red dashed line. Note that the axis for the cross sections is temperature-dependent and valid only for 140 K. In Ref. 74 at 140 K a line broadening coefficient for $J=2$ of γ of 0.079 cm^{-1}/atm is determined. The extrapolated value to 140 K from the alignment decay for the cross section $\sigma^c_{N_2-Ar}$ is 73.5 $Å^2$. This corresponds to a γ of 0.085 cm^{-1}/atm. Within the error bars, this again agrees with the depopulation rates measured by the broadening of the lines in the Raman Q-branch, and we can confirm the absence of pure dephasing also for the nitrogen-argon mixture at low temperature.

4. Nitrogen-krypton

We performed experiments on the nitrogen-krypton gas mixture at room temperature at a constant nitrogen partial pressure of 0.3 atm, while the krypton pressure was varied between 0.4 and 2.5 atm and at 120 K for a nitrogen partial pressure of 0.1 atm. For this system, measurements proved to be difficult and had to be performed at lower pump pulse intensity than the other experiments reported in this paper, as the onset of nonlinear processes due to the large electronic polarizability of krypton[78] leads to increased fluctuations. At room temperature we find a signal decay time τ_{hom} of 59 ps/atm, corresponding to a collision rate of ν_{N_2-Kr} of 0.0085 ps^{-1} atm^{-1}. The cross section $\sigma^c_{N_2-Kr}$ derived from the data is 63.9 $Å^2$. The decay time results in a hypothetical line broadening coefficient γ of 0.045 cm^{-1}/atm.

For a temperature of 120 K the decay time τ_{hom} for alignment is 32.6 ps/atm, corresponding to $\nu_{N_2-Kr}=0.015$ ps^{-1} atm^{-1} and $\sigma^c_{N_2-Kr}$ of 71.2 $Å^2$. From these data a line broadening coefficient γ of 0.081 cm^{-1}/atm is obtained. To the best of the authors' knowledge, no published data on the broadening of transition lines in the nitrogen-krypton system are available.

TABLE II. Lifetimes of the homodyne detected signal τ_{hom} in pure nitrogen and the gas mixtures, the collision rates of nitrogen with the respective partners ν_{N_2-X}, and the cross sections for rotational dephasing $\sigma^c_{N_2-X}$ derived from the signal decay of alignment. For comparison, we show the cross section for depopulation $\sigma^p_{N_2-X}$ derived from the literature values for γ for the $J=2$ rotational level, and the gas kinetic cross section σ^{kin} at room temperature.

	τ_{hom} (ps/atm)		ν_{N_2-X} ($ns^- atm^{-1}$)		$\sigma^c_{N_2-X}$ (Å^2)		$\sigma^p_{N_2-X}(J=2)$ (Å^2)	$\sigma^{kin}_{N_2-X}$ (Å^2)
	Low T	295 K	Low T	295 K	Low T	295 K	295 K	295 K
N_2-H_2	22.9±3 (77 K)	⋯	22±4	⋯	22.1±4	⋯	19.4[a] (17.8[a] at 77 K)	32[b]
N_2-He	43.7±4 (80 K)	71.5±8	11±2	7±1	18.1±3	21.3±3	19.1[c]	26.5[b]
N_2-N_2	15.6±2.5 (80 K)	64.9±5	36±6	8±1	102±5	48±8	57[d]	43[b]
N_2-Ar	22±3 (90 K)	65±6	22±3	8±1.5	80.5±8	51.1±8	56[e] (66[e] at 140 K)	40.8[b]
N_2-Kr	32.6±4 (120 K)	59±6	15±2	8.5±1.5	71.2±8	63.8±8	⋯	47.5[b]

[a]From Ref. 66.
[b]From Ref. 72.
[c]From Ref. 58.
[d]From Refs. 26 and 27.
[e]From Ref. 74.

V. DISCUSSION

We obtained the cross section for rotational decoherence from the evaluation of the signal decay of nonadiabatic alignment in nitrogen and mixtures of nitrogen with different perturbers. The results are collected together with the available literature data in Table II. In the nonadiabatic alignment a laser pulse, which is short compared to the rotational period of the molecule, imprints a common phase on all rotational transitions excited. At the half and full revival times, all rotations excited by the pump pulse line up in phase, due to the common divider of $2B$ in the rotational periods, and thus pronounced peaks of alignment or antialignment are observed. Upon a collision, rotational energy is redistributed among the collision partners, and the rotational motion acquires a random phase, even though the common factor of $2B$ in rotational energy is retained. With the collision times statistically distributed, the molecule is lost for the phase-sensitive revival amplitudes we use to quantify the decay of rotational coherence. The nonthermal M distribution resulting from the excitation with a linearly polarized laser creates additionally a time-independent alignment, as discussed in Refs. 35 and 36. Due to the relative smallness of this population part compared to the coherent oscillations under our experimental conditions,[22] however, it cannot be independently determined in the integrating approach to data analysis and does not affect our results.

First, we consider the rotational state dependence of the cross section for decoherence σ^c. The observed single-exponential decay of the homodyne detected alignment signal in all combinations indicates that σ^c does not depend significantly on J within the range relevant of $J=1$ to $J=5$ under our experimental conditions. The slow variation of σ^p with J found in theoretical approaches and Raman Q-branch experiments is illustrated in Fig. 8 and Figs. 10–13 and it supports this observation. The problem in this case reduces to a single cross section characterizing the response of all contributing J levels.

Next, we inspect the relation of σ^c to σ^p based on the comparison in Table II. In general, we find a good agreement for similar temperature between our set of σ^c values and the available σ^p values measured by different groups for all gas mixtures. For pure nitrogen and the nitrogen-argon mixture, our values are essentially within the error bars of the literature data or lower, only for the light collision partners hydrogen and helium, we find somewhat larger decoherence rates compared to the published depopulation data. The equality of σ^c and σ^p means that rotational coherence in these examples is destroyed in a $\Delta J \neq 0$ type of collision and pure dephasing with $\Delta J=0$ is insignificant. We can draw this conclusion for the range of pressures between 0.1 atm and 1 atm, corresponding to the binary collision regime of the dilute gas. At high densities, and especially in liquids, pure dephasing is expected to be of major importance. The equality of σ^c and σ^p holds in our experiments for the temperature range from close to liquefaction temperature of nitrogen (80 K) up to room temperature.

Finally, in Fig. 14, we compare our σ^c values to the gas kinetic cross section σ^{kin}. We use the standard cross sections at room temperature for pure perturbers from Ref. 58 and determine the combined cross section $\sigma^{kin}_{N_2-X}$ analogous to Eq. (13). The number of electrons Z and thus size and polarizability scale with the molecular mass m, and therefore the increase of $\sigma^{kin}_{N_2-X}$ in Fig. 14 is expected. To separate H_2 from

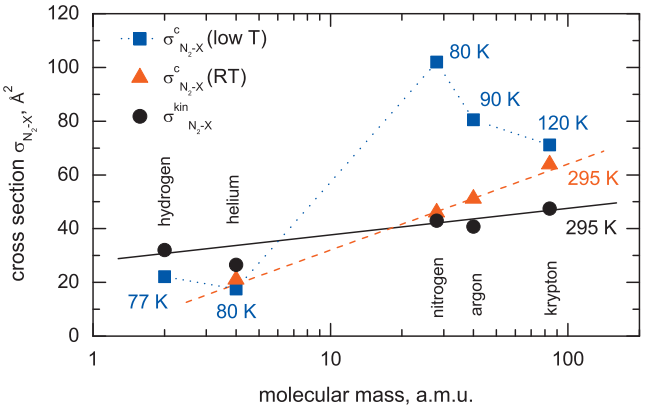

FIG. 14. Cross sections for decoherence $\sigma^c_{N_2-X}$ at low temperature (blue squares) and at room temperature (red triangles) as a function of the molecular mass of the collision partner. For comparison, the gas kinetic cross sections $\sigma^{kin}_{N_2-X}$ at room temperature are shown as black circles. The lines are guides to the eyes.

He, we plot the cross sections not as functions of Z, but rather as functions of molecular mass m, and use a semilogarithmic scale to better visualize the spread in m. In this scale, $\sigma^{\mathrm{kin}}_{\mathrm{N-2-}X}$ is increasing almost linearly (solid black line in Fig. 14), with only the He atom deviating toward a smaller value caused by the tighter binding of electrons in He. The $\sigma^{\mathrm{kin}}_{\mathrm{N_2-}X}$ values are compared to the $\sigma^{c}_{\mathrm{N_2-}X}$ values at room temperature, plotted as red triangles in Fig. 14 and connected by a straight dashed line as a guide to the eyes. For the N_2-N_2 system obviously, σ^{kin} and σ^{c} are almost identical. This leads to the very intuitive notion that the loss of rotational coherence requires a hard sphere collision. Figure 14 shows, however, that the dependence of the decoherence cross section on molecular mass is steeper than in the case of the gas kinetic cross section, and the lines describing the dependences cross coincidentally for the N_2-N_2 system. At both limits, consequently deviations toward larger as well as smaller values appear. Decoherence cross sections for the nitrogen-krypton system are larger than the gas kinetic cross section, while for the light perturbers hydrogen and helium σ^{kin} significantly exceeds σ^{c}. The loss of rotational coherence and population for the nitrogen-hydrogen and nitrogen-helium systems therefore requires more than one hard sphere collision. In the mechanistic picture of a collision event it is expected that a collision partner approaching in the rotational plane has a stronger impact than in the vertical direction.[79] This should be more strictly valid for the atomic perturbers which do not possess a plane of rotation themselves. Furthermore, the large rotational constant of 60 cm^{-1} of the hydrogen molecule, 30 times larger than for nitrogen, may inhibit the coupling of rotational degrees of freedom. This is supported by the fact that in our experiments para-hydrogen, predominantly in $J=0$, and normal hydrogen, predominantly in $J=1$ with a quadrupole moment, do not lead to a significant difference in the decay of rotational coherence. For the heavy Kr atom, the relative $Kr-N_2$ velocity decreases compared to the light perturbers, and the large σ^{c} in this case might be governed by the same mechanism as the temperature dependence we will discuss now.

The values for σ^{c} at low temperature are shown in Fig. 14 as blue squares, together with the temperature they were obtained at. The temperature varies between 77 K for hydrogen and 120 K for krypton to avoid liquefaction of one of the components. The effect of cooling on 58 $\mathrm{Å}^2$ for pure nitrogen is dramatic, with $\sigma^{c}_{\mathrm{N_2-N_2}}$ at 80 K exceeding the gas kinetic cross section σ^{kin} (295 K) by more than a factor of 2. Unfortunately no data on $\sigma^{p}_{\mathrm{N_2-N_2}}$ at low temperature are published. A similar strong increase is observed for the cross section for rotational relaxation σ^{r}.[30–33] The numerical value of σ^{r}, however, is much lower than either σ^{p} or σ^{c}, as the return to thermal equilibrium proceeds at a rate slower than individual collisions.[34] The growth in the cross sections with decreasing temperature results from the small translational velocities a low temperature. For low temperature, the long range attractive part of the intermolecular potential and so-called orbiting collisions[62–64] come into play and increase the cross section beyond the radius in the hard sphere model.

VI. CONCLUSIONS

The evaluation of the decay over time of the peak area of half and full revivals in the homodyne detected optical Kerr effect signal of alignment in nitrogen gas proved to be a direct way to determine the damping of rotational coherence. It allowed us to derive the relevant cross section $\sigma^{c}_{\mathrm{N_2-}X}$ for pure nitrogen and a variety of collision partners without relying on modeling. The cross section for decoherence for pure nitrogen shows a strong dependence on temperature, increasing by more than a factor of 2 upon lowering the temperature from room temperature to 80 K. This leads to the decay rate of molecular alignment becoming almost independent of temperature at a constant number density of the gas. The resulting stability of revivals with respect to temperature may be relevant for the implementation of quantum information schemes.

To measure the molecular alignment we used the optical Kerr effect method for pressures up to some atmospheres, however, the pressure range the method can be applied in has no fundamental limit. Even our analysis based on the integrated area of revival peaks allows to increase the pressure by an order of magnitude, and heterodyning instead of homodyning will slow down the decay of the signal. For higher pressure and liquids there exist a well developed set of methods for data analysis based on Fourier analysis.[41] The suitability for high pressure is an advantage compared to the frequency-domain Raman Q-branch method, where overlapping lines already at 1 atm pose a serious problem for data evaluation. Also, temperature is not a limitation, e.g., we have applied the Kerr effect method successfully to study dynamics in hydrogen at 10 K.[51] This flexibility, together with the excellent agreement of experiment and theory for alignment of diatomics at moderate laser intensities, makes it an ideal method to obtain values for the cross sections for rotational decoherence, which are important for the use of rotational revivals in spectroscopy, as well as in quantum information schemes. Rotational frequency resolution, if desired, could be obtained by shaping the composition of the rotational wave packets with suitably designed excitation pulse length.[22]

ACKNOWLEDGMENTS

The authors wish to express their gratitude for fruitful discussions to M. Héjjas and Dr. R. Püttner. The research was funded by Deutsche Forschungsgemeinschaft via Sonderforschungsbereich 450.

[1] T. Seideman and E. Hamilton, Adv. At., Mol., Opt. Phys. **52**, 289 (2005) (and references therein).
[2] H. Stapelfeldt and T. Seideman, Rev. Mod. Phys. **75**, 543 (2003) (and references therein).
[3] R. Velotta, N. Mason, M. Castillejo, and J. P. Marangos, Phys. Rev. Lett. **87**, 183901 (2001).
[4] D. Pavičić, K. F. Lee, D. M. Rayner, P. B. Corkum, and D. M. Villeneuve, Phys. Rev. Lett. **98**, 243001 (2007).
[5] P. J. Ho, D. Starodub, D. K. Saldin, V. L. Shneerson, A. Ourmazd, and R. Santra, J. Chem. Phys. **131**, 131101 (2009).
[6] E. R. Peterson, C. Buth, D. A. Arms, R. W. Dunford, E. P. Kanter, B. Krassig, E. C. Landahl, S. T. Pratt, R. Santra, S. H. Southworth, and L. Young, Appl. Phys. Lett. **92**, 094106 (2008).

[7] R. de Nalda, E. Heesel, M. Lein, N. Hay, R. Velotta, E. Springate, M. Castillejo, and J. P. Marangos, Phys. Rev. A **69**, 031804 (2004).
[8] J. Itatani, J. Levesque, D. Zeidler, H. Niikura, H. Pepin, J. C. Kieffer, P. B. Corkum, and D. M. Villeneuve, Nature (London) **432**, 867 (2004).
[9] B. K. McFarland, J. P. Farrell, P. H. Bucksbaum, and M. Gühr, Science **322**, 1232 (2008).
[10] T. Kanai, S. Minemoto, and H. Sakai, Nature (London) **435**, 470 (2005).
[11] W. Boutu, S. Haessler, H. Merdji, P. Breger, G. Waters, M. Stankiewicz, L. J. Frasinski, R. Taieb, J. Caillat, A. Marquet, P. Monchicourt, B. Carre, and P. Salieres, Nat. Phys. **4**, 545 (2008).
[12] Y. Mairesse, J. Levesque, N. Dudovich, P. B. Corkum, and D. M. Villeneuve, J. Mod. Opt. **55**, 2591 (2008).
[13] K. Hartinger, S. Nirmalgandhi, J. Wilson, and R. A. Bartels, Opt. Express **13**, 6919 (2005).
[14] H. Cai, J. Wu, A. Couairon, and H. Zeng, Opt. Lett. **34**, 827 (2009).
[15] T. Seideman, Phys. Rev. Lett. **83**, 4971 (1999).
[16] R. W. Robinett, Phys. Rep. **392**, 1 (2004).
[17] K. Ohmori, Annu. Rev. Phys. Chem. **60**, 487 (2009).
[18] M. Gühr, M. Bargheer, M. Fushitani, T. Kiljunen, and N. Schwentner, Phys. Chem. Chem. Phys. **9**, 779 (2007).
[19] M. Leibscher, I. S. Averbukh, and H. Rabitz, Phys. Rev. Lett. **90**, 213001 (2003).
[20] C. Z. Bisgaard, M. D. Poulsen, E. Peronne, S. S. Viftrup, and H. Stapelfeldt, Phys. Rev. Lett. **92**, 173004 (2004).
[21] S. Fleischer, I. S. Averbukh, and Y. Prior, Phys. Rev. Lett. **99**, 093002 (2007).
[22] N. Owschimikow, B. Schmidt, and N. Schwentner, Phys. Rev. A **80**, 053409 (2009).
[23] K. F. Lee, D. M. Villeneuve, P. B. Corkum, and E. A. Shapiro, Phys. Rev. Lett. **93**, 233601 (2004).
[24] E. A. Shapiro, M. Spanner, and M. Y. Ivanov, J. Mod. Opt. **52**, 897 (2005).
[25] D. J. Tannor, *Introduction to Quantum Mechanics: A Time-Dependent Perspective* (University Science Books, Sausalito, 2007).
[26] G. J. Rosasco, W. Lempert, W. S. Hurst, and A. Fein, Chem. Phys. Lett. **97**, 435 (1983).
[27] G. O. Sitz and R. L. Farrow, J. Chem. Phys. **93**, 7883 (1990).
[28] J. S. Murphy and J. E. Boggs, J. Chem. Phys. **47**, 691 (1967).
[29] A. Laubereau and W. Kaiser, Rev. Mod. Phys. **50**, 607 (1978).
[30] L. Abad, D. Bermejo, V. J. Herrero, J. Santos, and I. Tanarro, J. Phys. Chem. A **101**, 9276 (1997).
[31] F. J. Aoiz, T. Diez-Rojo, V. J. Herrero, B. Martinez-Haya, M. Menendez, P. Quintana, L. Ramonat, I. Tanarro, and E. Verdasco, J. Phys. Chem. A **103**, 823 (1999).
[32] G. J. Prangsma, A. H. Alberga, and J. J. M. Beenakker, Physica (Utrecht) **64**, 278 (1973).
[33] E. H. Carnevale, C. Carey, and G. Larson, J. Chem. Phys. **47**, 2829 (1967).
[34] J. G. Parker, Phys. Fluids **2**, 449 (1959).
[35] S. Ramakrishna and T. Seideman, Phys. Rev. Lett. **95**, 113001 (2005).
[36] S. Ramakrishna and T. Seideman, J. Chem. Phys. **124**, 034101 (2006).
[37] G. O. Sitz and R. L. Farrow, J. Chem. Phys. **101**, 4682 (1994).
[38] A. C. Eckbreth, P. A. Bonczyk, and J. F. Verdieck, Appl. Spectrosc. Rev. **13**, 15 (1977).
[39] D. Bassi, A. Boschetti, S. Marchetti, G. Scoles, and M. Zen, J. Chem. Phys. **74**, 2221 (1981).
[40] T. E. Gough and R. E. Miller, J. Chem. Phys. **78**, 4486 (1983).
[41] N. A. Smith and S. R. Meech, Int. Rev. Phys. Chem. **21**, 75 (2002).
[42] V. Renard, M. Renard, S. Guerin, Y. T. Pashayan, B. Lavorel, O. Faucher, and H. R. Jauslin, Phys. Rev. Lett. **90**, 153601 (2003).
[43] M. Morgen, W. Price, P. Ludowise, and Y. Chen, J. Chem. Phys. **102**, 8780 (1995).
[44] M. Morgen, W. Price, L. Hunziker, P. Ludowise, M. Blackwell, and Y. Chen, Chem. Phys. Lett. **209**, 1 (1993).
[45] B. Lavorel, O. Faucher, M. Morgen, and R. Chaux, J. Raman Spectrosc. **31**, 77 (2000).
[46] B. Friedrich and D. Herschbach, Phys. Rev. Lett. **74**, 4623 (1995).
[47] B. Friedrich and D. Herschbach, J. Phys. Chem. **99**, 15686 (1995).
[48] J. Ortigoso, M. Rodriguez, M. Gupta, and B. Friedrich, J. Chem. Phys. **110**, 3870 (1999).
[49] B. Schmidt and U. Lorenz (2009), WAVEPACKET 4.7: A program package for quantum-mechanical wavepacket propagation and time-dependent spectroscopy. Available via http://wavepacket.sourceforge.net.
[50] C. Horn, M. Wollenhaupt, M. Krug, T. Baumert, R. de Nalda, and L. Banares, Phys. Rev. A **73**, 031401(R) (2006).
[51] F. Königsmann, M. Fushitani, N. Owschimikow, D. T. Anderson, and N. Schwentner, Chem. Phys. Lett. **458**, 303 (2008).
[52] M. Born and E. Wolf, *Principles of Optics: Electromagnetic Theory of Propagation, Interference and Diffraction of Light*, 7th ed. (Cambridge University Books, Cambridge, 1999).
[53] J. O. Hirschfelder, C. F. Curtiss, and R. B. Bird, *Molecular Theory of Gases and Liquids* (Wiley, New York, 1954).
[54] K. Huber and G. Herzberg, *Molecular Spectra and Molecular Structure. IV. Constants of Diatomic Molecules*, 1st ed. (Van Nostrand, New York, 1979).
[55] D. W. Broege, R. N. Coffee, and P. H. Bucksbaum, Phys. Rev. A **78**, 035401 (2008).
[56] L. B. Loeb, *The Kinetic Theory of Gases* (Dover, New York, 1961).
[57] S. Green, J. Chem. Phys. **98**, 257 (1993).
[58] *CRC Handbook of Chemistry and Physics*, 84th ed., edited by D. R. Lide (CRC, Boca Raton, 2003).
[59] P. J. Agg and D. Clary, Mol. Phys. **73**, 317 (1991).
[60] L. A. Rahn and R. E. Palmer, J. Opt. Soc. Am. B **3**, 1164 (1986).
[61] G. Millot, J. Chem. Phys. **93**, 8001 (1990).
[62] J. N. L. Connor, Mol. Phys. **15**, 621 (1968).
[63] J. P. Toennies, W. Welz, and G. Wolf, J. Chem. Phys. **71**, 614 (1979).
[64] D. W. Chandler, J. Chem. Phys. **132**, 110901 (2010).
[65] I. A. Bocharova, H. Mashiko, M. Magrakvelidze, D. Ray, P. Ranitovic, C. L. Cocke, and I. V. Litvinyuk, Phys. Rev. A **77**, 053407 (2008).
[66] L. Gomez, D. Bermejo, P. Joubert, and J. Bonamy, Mol. Phys. **104**, 1869 (2006).
[67] L. Gómez, R. Z. Martínez, D. Bermejo, F. Thibault, P. Joubert, B. Bussery-Honvault, and J. Bonamy, J. Chem. Phys. **126**, 204302 (2007).
[68] P. Joubert, J. Bonamy, L. Gomez, and D. Bermejo, J. Raman Spectrosc. **39**, 707 (2008).
[69] G. Paterson, S. Marinakis, M. L. Costen, K. G. McKendrick, J. Klos, and R. Tobola, J. Chem. Phys. **129**, 074304 (2008).
[70] M. L. Costen, R. Livingstone, K. G. McKendrick, G. Paterson, M. Brouard, H. Chadwick, Y. P. Chang, C. J. Eyles, F. J. Aoiz, and J. Klos, J. Phys. Chem. A **113**, 15156 (2009).
[71] M. Brouard, H. Chadwick, Y. P. Chang, R. Cireasa, C. J. Eyles, A. O. L. Via, N. Screen, F. J. Aoiz, and J. Klos, J. Chem. Phys. **131**, 104307 (2009).
[72] K. S. Jammu, G. E. St. John, and N. L. Welsh, Can. J. Phys. **44**, 797 (1966).
[73] A. E. Belikov, R. G. Sharafutdinov, and A. V. Storozhev, Chem. Phys. **213**, 319 (1996).
[74] D. N. Kozlov, R. L. Pykhov, V. V. Smirnov, K. A. Vereschagin, A. I. Burshtein, and A. V. Storozhev, J. Raman Spectrosc. **22**, 403 (1991).
[75] R. L. Farrow and L. A. Rahn, J. Opt. Soc. Am. B **2**, 903 (1985).
[76] M. D. Pattengill, R. A. La Budde, R. B. Bernstein, and C. F. Curtiss, J. Chem. Phys. **55**, 5517 (1971).
[77] P. G. Kistemaker and A. E. de Vries, Chem. Phys. **7**, 371 (1975).
[78] A. Couairon and A. Mysyrowicz, Phys. Rep. **441**, 47 (2007).
[79] M. L. Costen, S. Marinakis, and K. G. McKendrick, Chem. Soc. Rev. **37**, 732 (2008).